

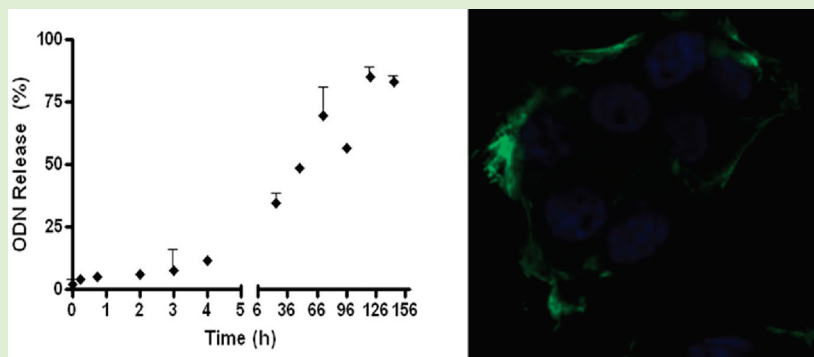
Slow Release and Delivery of Antisense Oligonucleotide Drug by Self-Assembled Peptide Amphiphile Nanofibers

Selma Bulut, Turan S. Erkal, Sila Toksoz, Ayse B. Tekinay,* Turgay Tekinay,* and Mustafa O. Guler*

UNAM-Institute of Materials Science and Nanotechnology, Bilkent University, Ankara 06800, Turkey

S Supporting Information

ABSTRACT:



Antisense oligonucleotides provide a promising therapeutic approach for several disorders including cancer. Chemical stability, controlled release, and intracellular delivery are crucial factors determining their efficacy. Gels composed of nanofibrous peptide network have been previously suggested as carriers for controlled delivery of drugs to improve stability and to provide controlled release, but have not been used for oligonucleotide delivery. In this work, a self-assembled peptide nanofibrous system is formed by mixing a cationic peptide amphiphile (PA) with *Bcl-2* antisense oligodeoxynucleotide (ODN), G3139, through electrostatic interactions. The self-assembly of PA-ODN gel was characterized by circular dichroism, rheology, atomic force microscopy (AFM) and scanning electron microscopy (SEM). AFM and SEM images revealed establishment of the nanofibrous PA-ODN network. Due to the electrostatic interactions between PA and ODN, ODN release can be controlled by changing PA and ODN concentrations in the PA-ODN gel. Cellular delivery of the ODN by PA-ODN nanofiber complex was observed by using fluorescently labeled ODN molecule. Cells incubated with PA-ODN complex had enhanced cellular uptake compared to cells incubated with naked ODN. Furthermore, *Bcl-2* mRNA amounts were lower in MCF-7 human breast cancer cells in the presence of PA-ODN complex compared to naked ODN and mismatch ODN evidenced by quantitative RT-PCR studies. These results suggest that PA molecules can control ODN release, enhance cellular uptake and present a novel efficient approach for gene therapy studies and oligonucleotide based drug delivery.

1. INTRODUCTION

Use of antisense oligonucleotides as inhibitors to regulate expression of specific genes is a promising approach for treatment of diseases such as cancer and infectious and inflammatory diseases.^{1,2} Antisense therapy has important advantages such as target specificity and reduced side effects. In theory, antisense molecules can be designed to inhibit expression of any gene.³ However, stability of these oligonucleotides in plasma is a problem, and there is ongoing research to improve their stability. Chemically modified oligonucleotides have improved stability, however, when they are not combined with proper delivery agents, they have limited ability to cross the cell membrane due to their charge and high molecular weight.^{4,5} Thus, effective delivery systems are necessary for enhanced cellular uptake. To achieve sustained pharmacological activity of oligonucleotides and to avoid multiple administrations, several release and delivery

systems based on biodegradable polymers or lipids have been suggested such as cationic liposomes,^{6,7} synthetic biodegradable polymers, nano or microparticles (polylactide-*co*-glycolide microparticles),^{8,9} hydrogels (PLA-*b*-PEG-*b*-PLA hydrogel),¹⁰ micelles (polylactide-polyethylene glycol copolymers),¹¹ fibrous scaffolds (electrospun polyethylene covinylacetate), polylactic acid,¹² and cationic polymers (polyethylenimine,¹³ polylysine,¹⁴ cationic facial amphiphiles¹⁵). These nonviral delivery systems are usually hydrophilic and positively charged.¹⁶ Nonviral delivery vectors constructed with biodegradable materials are preferred over viral delivery vehicles due to side effects of the latter such as non-specific toxicity and low performance in serum.¹⁷ The nonviral

Received: May 11, 2011

Revised: June 27, 2011

Published: June 28, 2011

systems mentioned above decrease enzymatic degradation of chemically unmodified oligonucleotides and partially increase their cellular uptake. However, these systems are generally difficult to use and mostly do not work in serum containing media. Furthermore, highly positively charged polymers such as polyethylenimine (PEI) cause cellular toxicity.¹⁸

Peptide amphiphiles (PAs), which are composed of a hydrophobic site, a β -sheet forming short peptide sequence, a hydrophilic peptide sequence, and a bioactive peptide group, are promising tools for drug and gene delivery systems because they are biocompatible and bioactive. PA molecules form highly ordered nanostructures through self-assembly. Hydrophobic site of PA molecules, composed of a long alkyl chain, induces hydrophobic collapse and remains in the interior part of the nanofiber structure. Hydrophilic peptide segment enables solubility in water and presents bioactive peptide sequence on the surface of the self-assembled nanostructures.^{19,20} The β -sheet structures are formed through intermolecular hydrogen bonding between peptides, oriented parallel along the axis of the well-defined, one-dimensional nanofiber structure.^{20–23} The addition of oppositely charged molecules such as biomacromolecules (e.g., DNA, protein, polysaccharides), divalent ions or change in pH trigger spontaneous nanofiber assembly of PAs through charge screening. Water absorption by the mesh-like network formed by these nanofibers results in gel structure.²⁴ Chemical, physical, and biological properties of nanofibers can be controlled by non-covalent bonds and supramolecular interactions.²⁵ Gels formed by PAs have been used for various applications including drug delivery. They were functionalized to release proteins such as sonic hedgehog (SHH) protein²⁶ or to deliver growth factors (e.g., bone morphogenic protein factor-2²⁷ and fibroblast growth factor²⁸). PA nanofibers were also employed to deliver and encapsulate hydrophobic drugs including pyrene,²⁹ doxorubicin,³⁰ and cisplatin.³¹

Positively charged carrier systems for oligonucleotide delivery have been used to provide effective cellular uptake through enhanced binding to negatively charged proteoglycans on the cell surface.^{32,33} Besides, hydrophobic content of the PA molecules facilitates internalization through cell membrane.³⁴ In this study, the hydrophilic lysine residues were chosen to bind to oligonucleotides and form nanofibers at physiological pH upon addition of oligonucleotides through charge screening. An amphiphilic peptide forming β -sheet structure with four nonpolar amino acid residues and positively charged lysine residue at physiological conditions was designed and synthesized to interact with oligonucleotides. Polyamine groups presented on the surface of the self-assembled nanofibers provide a positive charge at physiological pH that can facilitate uptake of PA-oligonucleotide complexes.^{35,36} Oligonucleotides can be released by degradation of the biodegradable peptide scaffold or by physical release mechanisms governed by diffusion. Cells can uptake nanofibers degraded by proteases and use them in their metabolic pathways showing biocompatibility of PAs.³⁷

Herein, we demonstrate self-assembled nanofiber formation of a PA system with an oligonucleotide as a slow release and delivery system. We demonstrate a new carrier system to deliver G3139 as an antisense oligonucleotide drug model. G3139 (Genasense, Genta Inc., NJ) is a chemically modified 18-mer phosphorothioate antisense oligodeoxynucleotide (ODN), designed to bind to the first six initiation codons of the *Bcl-2* mRNA.³⁸ *Bcl-2* protein family is crucial for mediating controlled cell death and overexpression of *Bcl-2* protein leads to accumulation

of aged and damaged cells resulting in tumor formation. *Bcl-2* has been associated with many aggressive tumor phenotypes.³⁹ G3139 has been shown to effectively reduce both *Bcl-2* mRNA and protein expression and induce programmed cell death.⁴⁰ G3139 has been in clinical trials since 1995 in the U.S.A., Europe and Australia, with efficacy and safety data from phases 1, 2, and 3 clinical trials. G3139 is now being evaluated clinically in treatment of melanoma, chronic lymphocytic leukemia, and other tumors in combination with many types of anticancer therapies.^{41–43}

In this study, we used a cationic peptide amphiphile molecule, Lys-PA (C₁₂-VVAGK-Am), as a nonviral antisense oligonucleotide carrier and delivery system. Controlled release of ODN from PA-ODN system, ODN internalization by cells and effects of this nanocarrier system on *Bcl-2* mRNA levels are demonstrated. We illustrated that PA and ODN molecules form nanofibers through charge screening by using circular dichroism, SEM, and AFM imaging. We showed that PA-ODN assembly provides controlled release of ODN from peptide nanofibers, enhanced intracellular accumulation of ODN and downregulation of *Bcl-2* mRNA.

2. EXPERIMENTAL SECTION

2.1.1. Materials. 9-Fluorenylmethoxycarbonyl (Fmoc) and *tert*-butoxycarbonyl (Boc)-protected amino acids, [4- α -(2',4'-dimethoxyphenyl)Fmoc-aminomethyl]phenoxy]acetamidonorleucyl-MBHA resin (Rink amide MBHA resin), and 2-(1*H*-benzotriazol-1-yl)-1,1,3,3-tetramethyluronium hexafluorophosphate (HBTU) were purchased from NovaBiochem and ABCR. DMEM media, fetal bovine serum (FBS), trypsin EDTA, and penicillin/streptomycin were purchased from Invitrogen.

2.1.2. Antisense Oligonucleotides. G3139, a phosphorothioate oligodeoxynucleotide (Genasense), with a sequence complementary for the first six codons of the open reading frame of *Bcl-2* mRNA: 5'-tct ccc agc gtc cgc cat-3' (18-mer) was used as the antisense ODN. A two-base mismatched (MM) sequence, G4126, 5'-tct ccc agc atg tgc cat-3', was used as control and G3139 labeled with 6-fluorescein on the 5'-t, G4243, 5'-tac cgc gtc cga ccc tct-3', was used in cell internalization assays. ODNs were donated by Genta Inc. (Genta Inc., NJ).

2.1.3. Cells. The human breast cancer cell line MCF-7 (American Type Culture Collection) was maintained in low glucose DMEM (GIBCO) supplemented with 10% FBS, 100 μ g/mL streptomycin, and 100 μ g/mL penicillin at 37 °C in a humidified incubator with 5% CO₂.

2.2. Peptide Synthesis, Purification, and Characterization.

2.2.1. Synthesis of Peptide Amphiphiles. Lauryl-VVAGK peptide (Lys-PA) was constructed on MBHA Rink Amide resin at 0.25 mmol scale. Amino acid couplings were done with 2 equiv of Fmoc-protected amino acid, 1.95 equiv of HBTU, and 3 equiv of DIEA for 2 h. Fmoc removal was performed with 20% piperidine/dimethylformamide (DMF) solution for 20 min. Cleavage of the peptides from the resin was carried out with a mixture of TFA:TIS:H₂O in the ratio of 95:2.5:2.5 for 3 h. Excess TFA was removed by rotary evaporation. The remaining viscous peptide solution was triturated with ice-cold ether and the resulting white product was freeze-dried. Peptide was characterized by liquid chromatography–mass spectrometry (LC-MS). Its purity was observed to be over 95% by LC chromatogram (Figures S1 and S2). Mass spectrum was obtained with Agilent LC-MS equipped with Zorbax SB-C8 4.6 \times 100 mm column. A gradient of (a) water (0.1% formic acid) and (b) acetonitrile (0.1% formic acid) was used for LC-MS characterization. Peptide purification was performed with a Zorbax prepHT 300SB-C8 column with water–acetonitrile (0.1% TFA) gradient.

2.2.2. Circular Dichroism (CD) Measurement. JASCO J815 CD spectropolarimeter was used at RT to analyze secondary structures in 400 μL of peptide solution alone at a final concentration of 3.8×10^{-4} M and mixture of peptide (3.8×10^{-4} M final) and ODN (3.125 μM final) solutions at wavelengths ranging from 260 to 190 nm, data interval and data pitch being 0.1 nm, scanning speed being 100 nm/min. All measurements were done with three accumulations. DIT was selected as 1 s, bandwidth as 1 nm, and the sensitivity was standard.

2.2.3. Viscoelasticity and Gelation Behavior. Gelation behaviors of the ODN and Lys-PA gels were evaluated by an Anton Paar Physica RM301 Rheometer operating with a 25 mm parallel plate configuration at 25 °C. Each sample with 100 μL of total volume with a final peptide concentration of 1 wt % and ODN solutions with different concentrations was carefully loaded on the center of the lower plate and incubated for 15 min before performing rheometry analysis. After equilibration, the upper plate was lowered to a gap distance of 0.5 mm. Storage moduli (G') and loss moduli (G'') values were measured from 100 rad/s to 0.1 rad/s of angular frequency with 0.5% shear strain.

2.2.4. Morphological Observation. Three-dimensional network of the nanofibrous gel was observed by atomic force microscopy (AFM) and scanning electron microscopy (SEM).

2.2.4.1. Atomic Force Microscopy (AFM). AFM sample was prepared by mixing 0.02 wt % PA and ODN solution in H_2O . After incubation for 30 min at RT, the mixture was diluted 20 \times in H_2O to obtain 0.5 μM ODN concentration. Final solution was drop-casted and dried on a freshly cleaved silicon wafer. AFM images were recorded using model MFP-30 from Asylum Research operated in tapping mode at a frequency of 246 kHz. AFM images were taken at 1024 \times 512 pixels resolution. Image was taken with spring constant 40 N/m and the set point and scanning speed were 0.7–1.0 V and 1.0–1.5 Hz, respectively.

2.2.4.2. Scanning Electron Microscopy (SEM). A 3D network of self-assembled 100 μL gels were prepared on a metal mesh by mixing 50 μL of 1 wt % PA solution in H_2O with 50 μL of ODN solution in PBS (1 \times , pH 7.4) containing 250 ng/ μL of ODN. Water was exchanged with ethanol gradually in water/ethanol mixtures of increasing ethanol concentrations and finally in 100% ethanol for 30 s at each step. Gel was dried at critical point (1072 psi, 31 °C) with Tousimis Autosamdri-815B, Series C critical point dryer and coated with 10 nm Au–Pd. Sample was imaged by a FEI Quanta 200 FEG, using the ETD detector at high vacuum mode at a voltage of 30 keV.

2.3. ODN Release from PA-ODN Gel. ODN release from PA-ODN gel was examined by diluting Lys-PA with H_2O to 2 wt % in 50 μL and mixing with 50 μL of ODN solution (30 $\mu\text{g}/\mu\text{L}$ and 2 $\mu\text{g}/\mu\text{L}$) in PBS (1 \times , GIBCO) to obtain a final 1 wt % peptide gel containing 15 $\mu\text{g}/\mu\text{L}$ and 1 $\mu\text{g}/\text{mL}$ ODN. After 15 min incubation, 100 μL of 1 \times PBS was added onto gel. ODN release was measured by NanoDrop (The Thermo Scientific NanoDrop 2000, U.S.A.) at 260 nm for a period of 6 days for gel formed with 30 $\mu\text{g}/\mu\text{L}$ ODN and 3 days for gel formed with 2 $\mu\text{g}/\mu\text{L}$ ODN solution. To examine the effect of PA and ODN concentration on release profile of ODN; 100 μL of gels were formed using ODN with concentrations of 150–1200 ng/ μL and PA with concentrations of 0.2–0.1 wt %. The gels were prepared in 96-well plates and incubated for 1 h at 37 °C followed by overnight drying in a laminar flow hood. Next day, 100 μL of PBS (1 \times) was added on coated wells and gels were maintained at 37 °C for a period of 5 days during ODN concentration analysis. To see burst release, 2 μL aliquots from PBS solution were measured in short time intervals during the first day and every 24 h afterward. A total of 2 μL of fresh buffer was added to wells after each measurement for all experiments. ODN release versus time was graphed according to initial concentration of ODN trapped in the gel. Three replicates were tested for each PA and ODN formulation.

2.4. Cellular Uptake of PA-ODN Complexes. MCF-7 breast cancer cells (3×10^4 cells/well) were plated in 0.5 mL of growth medium on coverslips in 24-well chambered plates and grown overnight.

On the following day, the cells were treated with 20 μL of mixture with an equal volume of Lys-PA and FAM-labeled ODN (G3139) or 10 μL of FAM labeled ODN alone for 4 h. Mixture of FAM labeled ODN (30 ng/ μL) in PBS and 0.01 wt % Lys-PA in H_2O was prepared by gently mixing ODNs and PAs to achieve a molar ratio of 30:1 (Lys-PA/ODN), followed by incubation for 30 min at RT. After 4 h incubation, cells were rinsed three times with PBS, fixed with 4% paraformaldehyde and stained with 1 $\mu\text{g}/\text{mL}$ solution of TO-PRO-3 (Invitrogen) for nuclei staining. To see the distribution of the PA-ODN complex in cell cytoplasm, after a 4 h incubation with FAM-labeled ODN alone or PA-ODN mixture, cell culture medium was removed, 500 $\mu\text{L}/\text{well}$ fresh cell culture medium was added, and cells were incubated for an additional 44 h. Cells were imaged by a laser scan confocal microscope (ZEISS LSM 510 META, ZEISS GmbH, Jena, Germany).

2.4.1. Cell Viability and Proliferation Assay. The cytotoxicity of the ODN, PA, and PA-ODN complexes was measured by MTT [3-(4,5-dimethylthiazol-2-yl)-2,5-diphenyl tetrazolium bromide] assay (Sigma). MCF-7 cells were plated on 96-well plates at a density of 3×10^3 cells/well and grown overnight. Next day, the cells were treated with either a 5 μL mixture of equal volumes of Lys-PA (0.02 wt %) and ODN/MM-ODN or a 2.5 μL of 1 μM solution of ODN/MM-ODN alone. After incubation at 37 °C for 4 h, cell culture medium was replaced with fresh medium followed by additional 44 h incubation. MTT assay was performed according to the manufacturer's protocol. Briefly, media on cells were aspirated and 100 μL fresh media containing 10% (v/v) reconstituted MTT (M-5655) reagent was added to each well. The plates were incubated for 3 h and the absorbance of the medium was measured at 570 nm with plate reader (SpectraMax MS, Molecular Devices). The background absorbance of multiwell plates were also measured at 690 nm and subtracted from the 570 nm measurement.

To confirm the effect of PA-ODN complex on proliferation of MCF-7 cells, the BrdU cell proliferation kit (Roche) was used. Cells were seeded at a density of 3000 cells/well in a final volume of 100 μL in 96-well culture dishes and incubated overnight. The cells were treated with either a 5 μL mixture of equal volumes of Lys-PA (0.02 wt %) and ODN/MM-ODN or a 2.5 μL solution of ODN/MM-ODN alone with 1 μM final concentration. After incubation at 37 °C for 4 h, cell culture medium was changed with fresh medium followed by additional 20 h incubation. Next, 10 μL of 100 μM BrdU label was added to each well and incubated for an additional 24 h at 37 °C. The labeling medium was removed by tapping off and replaced with 200 μL of fix/denaturing solution followed by a 30 min incubation at RT. The fix/denaturing solution was removed thoroughly by flicking off and tapping. A total of 100 $\mu\text{L}/\text{well}$ anti-BrdU-POD working solution was added to each well and left for 90 min at RT. Antibody conjugate was removed by flicking off and wells were rinsed 3 times with 200–300 $\mu\text{L}/\text{well}$ with washing solution (PBS, 1 \times). Finally, 100 $\mu\text{L}/\text{well}$ of substrate solution was added into wells and incubated at RT until color development is sufficient for photometric detection (30 min). Absorbance (A370–A492 nm) of the samples was measured with plate reader (SpectraMax MS, Molecular Devices). Absorbance values were normalized with respect to cells incubated without ODN drug. Assays were carried out in triplicate.

2.4.2. Determination of Bcl-2 mRNA Expression by Quantitative RT-PCR. MCF-7 breast cancer cells were plated in six-well plates containing 2 mL of media. Following overnight growth at 37 °C in a humidified incubator with 5% CO_2 , cells were treated with either a 100 μL mixture of equal volumes of Lys-PA (0.02 wt %) and ODN/MM-ODN or a 50 μL solution of ODN/MM-ODN alone with 1 μM final concentration. After incubation at 37 °C for 4 h, cell culture medium was changed with fresh medium followed by additional 44 h incubation. The PA-ODN complexes were prepared by mixing equal volumes of ODN solution in PBS (1 \times , GIBCO) and Lys-PA (0.02 wt %) in dd H_2O and incubated for 30 min at RT before adding 5 μL of this mixture onto cells. After 4 h incubation with ODN, mismatch ODN or their complexes with

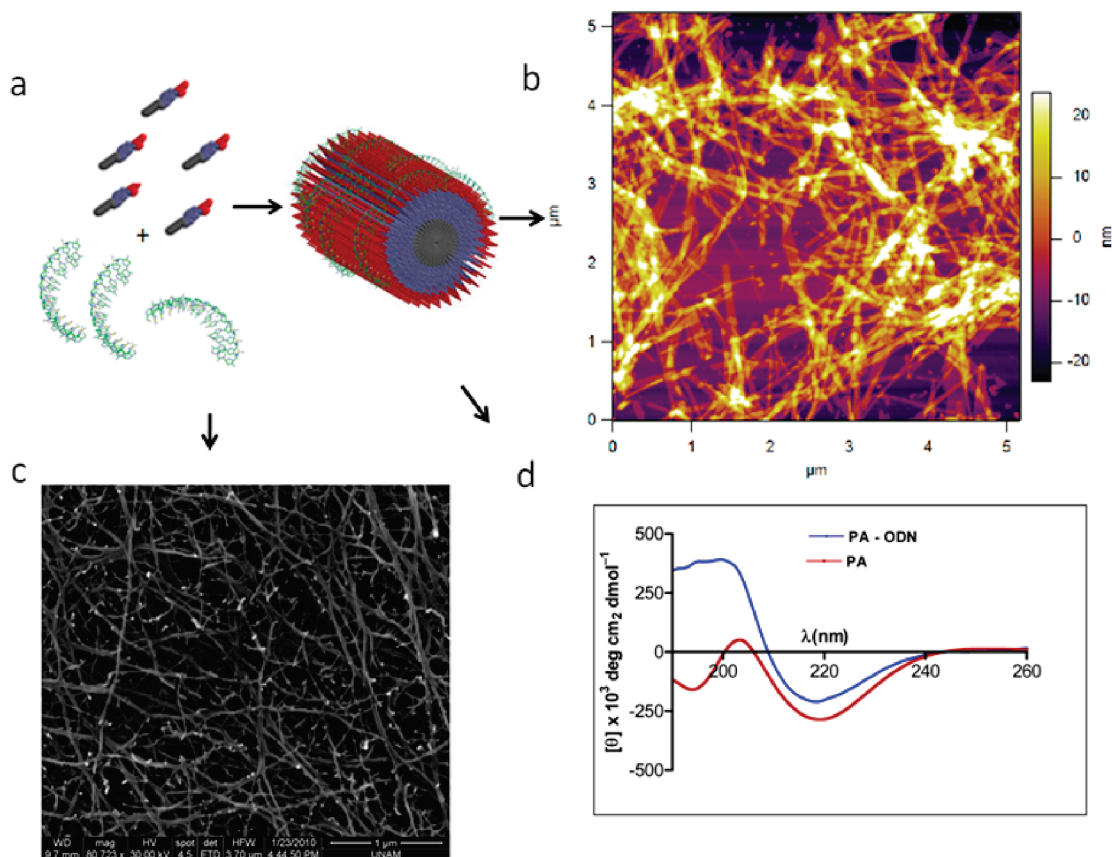


Figure 1. (a) Schematic representation of Lys-PA and ODN (5'-tct ccc agc gtg cgc cat-3') nanofibers. (b, c) AFM topography and SEM images of the nanofiber network reveal nanofibrous 3-D network of the PA-ODN complex. (d) CD spectra demonstrate increased β -sheet formation in PA-ODN mixture compared to PA alone.

Lys-PA, medium was replaced with fresh cell medium. Total RNA was extracted from cells after 48 and 72 h incubations by using Trizol reagent (Invitrogen). RNA concentration was measured with NanoDrop spectrophotometer (Thermo Scientific NanoDrop 2000, USA) at 260 nm.

The *Bcl-2* mRNA expression level was measured by using quantitative RT-PCR with SuperScript III Platinum SYBR Green One-Step qRT-PCR Kit (Invitrogen). Samples were incubated in C1000TM thermal cycler (CFX96 real Time systems, Bio-RAD). After cDNA synthesis for 3 min at 50 °C, cDNA denaturation was carried out for 5 min at 95 °C followed by denaturation at 95 °C for 15 s and annealing at 60 °C for 30 s. Primer sequences were designed by using DNASTAR Lasergene 8 program. The following primer pairs were used for qRT-PCR experiments: 5'-tgc ccc tgt gga tga ctg ag-3' and 5'-gtt tgg ggc agg cat gtt gac t-3' for *Bcl-2* and 5'-tcg aca gtc agc cgc atc ttc t-3' and 5'-gtg acc agg cgc cca ata cga c-3' for GAPDH. Relative gene expression values were determined by the Pfaffl method. GAPDH was used as housekeeping gene to normalize the gene expression levels of each sample.

2.4.3. Western Analysis. MCF-7 breast cancer cells were plated in six-well plates containing 2 mL of media. Following overnight growth at 37 °C in a humidified incubator with 5% CO₂, cells were treated with either a 100 μ L mixture of equal volumes of Lys-PA (0.02 wt %) and ODN/MM-ODN or a 50 μ L solution of ODN/MM-ODN alone with a final concentration of 1 μ M. After incubation at 37 °C for 4 h, cell culture medium was changed with fresh medium followed by additional 68 h incubation. The complexes of PA-ODN were prepared by mixing equal volumes of ODN solution in PBS (1 \times , GIBCO) and Lys-PA (0.02 wt %) in ddH₂O and incubated for 30 min at RT before adding of this mixture onto cells. After 72 h incubation, MCF-7 cells were washed

with 1 \times PBS and lysed with 100 μ L of 1 \times SDS-sample buffer. The extract was transferred to a microcentrifuge tube and centrifuged at 13000g for 10 min at 4 °C. The supernatant was collected to a fresh tube and the total protein concentration was determined by using BCA protein assay (Pierce, Rockford, IL). Cell lysates containing 50 μ g of total protein were loaded and separated on a 10% SDS-polyacrylamide gel at 150 V for 1.5 h. After blotting (trans-blot SD, Semi Dry transfer cell, Bio-Rad) to polyvinylidene difluoride membranes (Thermo Scientific) at 14 V for 35 min, the membrane was blocked in a solution of 5% powdered nonfat milk in Tris-buffered saline/Tween-20 followed by incubation with monoclonal anti-*Bcl-2* clone 100 (Millipore; 1:1000) or monoclonal anti- β -Actin antibody (1:5000; Sigma-Aldrich). After washing with milk, the membranes were incubated with horseradish peroxidase conjugated goat antimouse secondary antibody (Millipore) (1:2000). The membranes were developed with Novex Chemiluminescent Substrates (Invitrogen) and observed with Kodak Biomax NS film.

3. RESULTS AND DISCUSSION

Lauryl-VVAGK-Am (Lys-PA) peptide was synthesized by utilizing solid phase peptide synthesis method (Figures S1 and S2). Lauric acid provides amphiphilicity with its hydrophobic character that triggers peptide molecules to self-assemble into nanofibers. The β -sheet forming group consists of four nonpolar amino acid residues. Lysine residue provides water solubility and a cationic feature which triggers gel formation upon mixing with negatively charged oligonucleotides (Figure 1a). Characterization of PA-ODN gels by AFM and SEM imaging revealed their

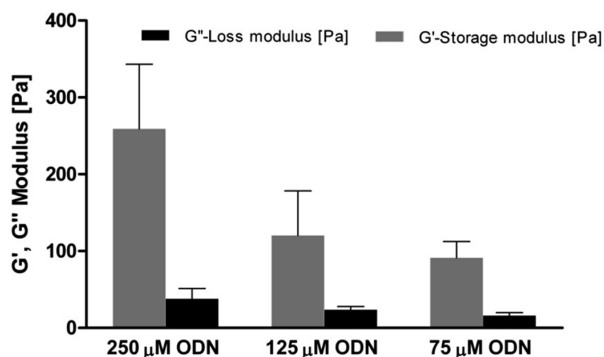


Figure 2. Storage (G') and loss (G'') moduli of gels indicate that Lys-PA (2 wt %) with varying concentrations of ODN form gel with viscoelastic character confirmed by greater G' values than G'' . Data points are average of $n = 3$ and error bars represent standard error of mean.

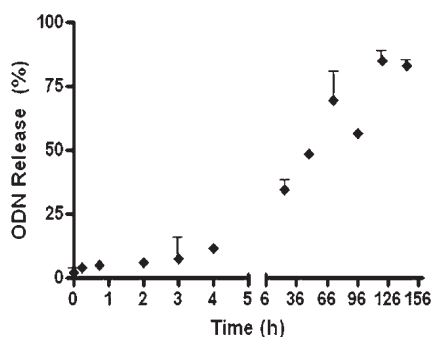


Figure 3. Release profile shows that there is sustained release of ODN from peptide nanofiber gel of $30 \mu\text{g}/\mu\text{L}$ ODN and 2 wt % PA for 6 days. Data points are average of $n = 3$ and error bars represent standard error of mean.

3-D nanofibrous network structure (Figure 1b,c). Lys-PAs self-assemble into nanofibers upon addition of oppositely charged ODN through charge screening and three-dimensional network of these nanofibers results in gel formation upon water encapsulation. Network formation is critical for drug release since it enables physical encapsulation of the drug in addition to electrostatic interactions between the ODN and PA molecules. In addition, ODN release is dependent on electrostatic interactions between the PAs and ODNs. Therefore, PA degradation can also be responsible for additional ODN release in vitro and in vivo.

Secondary structures of the nanofibers formed through charge neutralization of the PA molecules by mixing with ODNs were analyzed by circular dichroism (CD). CD spectroscopy at different concentrations of ODNs demonstrated PAs forming predominantly β -sheet structure at a concentration of 3.8×10^{-4} M. The β -sheets display a negative minimum at 218 nm and a positive ellipticity at 195 nm.⁴⁴ CD spectrum of PA without ODN at the same concentration revealed a mixture of random coil and β -sheet structures.⁴⁵ The amount of β -sheet structures in PA alone samples was much lower compared to CD spectrum of PA with ODN (Figure 1d).

Encapsulation of water by the 3-D nanofibrous network resulted in gel formation triggered by addition of ODN solution as demonstrated by oscillatory rheology. G' and G'' did not change

with angular frequency from 100 to 0.1 rad/s (Figure S3). As we increased the ODN amount, storage moduli (G') of samples increased and became significantly higher than their loss moduli (Figure 2). G'/G'' was higher than 1, a critical point of gelation, which indicates PA-ODN gel behaves like an elastic solid.²⁴

We evaluated the effect of the Lys-PA and ODN concentrations on the release of ODN through release assays. The nanofibrous nature of the PA-ODN system enables physical encapsulation of the ODN as well as increasing the physical interaction between the PA and ODN molecules. The release profile of ODN from gel prepared (Figure S4) by mixing $50 \mu\text{L}$ of 2 wt % Lys-PA and $50 \mu\text{L}$ of $30 \mu\text{g}/\mu\text{L}$ ODN is shown in Figure 3. We monitored sustained release of ODN from 3-D PA-ODN nanofibrous network while the majority of ODN (80–90%) was released by 6 days (Figure 3). Effect of charge ratio is an important factor that determines the strength of the electrostatic interactions and it was further studied by changing peptide concentration in the PA-ODN gels. For this purpose, ODN release was studied with a gel of $2 \mu\text{g}/\mu\text{L}$ ($2000 \text{ ng}/\mu\text{L}$) ODN and 2 wt % Lys-PA for 3 days (Figure S5). Release of ODN from gel formed with $30 \mu\text{g}/\mu\text{L}$ ODN solution was around 55% by day 3 while release of ODN from gel formed with $2 \mu\text{g}/\mu\text{L}$ ODN was around 15% with a slower release profile. In addition, Figure 4 demonstrates that ODN release from gel decreased as the peptide concentration was increased due to enhanced attraction of anionic ODNs by the cationic nanofibrous network. The average release profile was also affected by the concentration of ODN in gel, where the higher the ODN concentration, the higher ODN release from gel was observed due to insufficient attraction by cationic Lys-PAs on anionic ODNs in the gel. At low ODN concentrations ($150 \text{ ng}/\mu\text{L}$ and $300 \text{ ng}/\mu\text{L}$ in Figure 4a,b, respectively), 66% of the initial amount of ODN was trapped in the 0.1 and 0.2 wt % Lys-PA-ODN gels and release from the 3-D network was slow for all three concentrations of PAs. Release assay from the gels with $600 \text{ ng}/\mu\text{L}$ ODN concentration showed rapid initial release within the first 3 h when 0.1 wt % gel was used whereas slower release profiles were observed from 0.15 wt % and 0.2 wt % gels (Figure 4c). When a higher concentration ($1200 \text{ ng}/\mu\text{L}$) of ODN was used for release assays, rapid initial release within the first 3 h was observed for all three PA concentrations (Figure 4d). After 2 days, release profile reached plateau values for all formulations. When same PA concentration was used for encapsulating different concentrations of ODN, using lower concentrations of ODN resulted in slower release while as ODN concentrations were increased, more rapid initial release profiles were observed (Figure S6). Antisense oligonucleotides are not only localized on the surface of the nanofibers through electrostatic interactions between positively charged PA molecules and negatively charged ODNs but also physically encapsulated inside the peptide nanofiber network. The initial burst release is due to weaker interactions between the ODNs and the PAs which is caused by physical encapsulation. The latter slow release is likely to be caused by stronger bonds caused by electrostatic interactions between the PA and ODN molecules. Therefore, self-assembled PA and ODN nanofibers can be used for controlled ODN release by changing PA/ODN charge ratio and the PA-ODN nanofiber network provides a promising tool for controlled release of oligonucleotides. It is known that oligonucleotides have short half-lives in the body. Consequently, agent-free antisense ODN (G3139) is generally applied by continuous intravenous infusion. Thus, utilization of an effective delivery system is required to improve efficacy of gene targeted

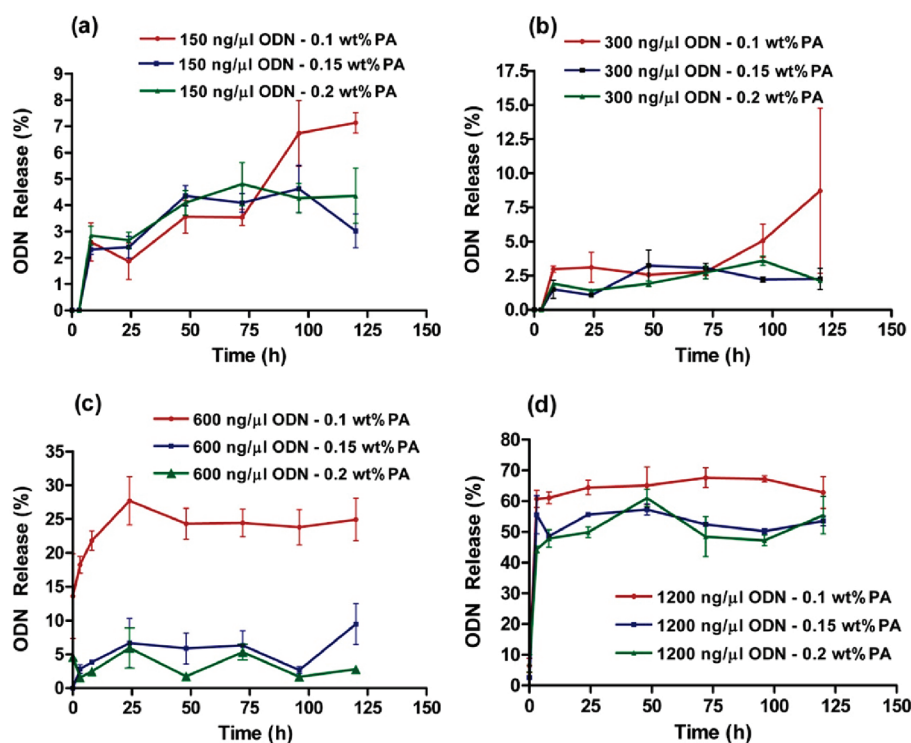


Figure 4. Release profile of ODN from gel of 0.1, 0.15, and 0.2 wt % PA and ODN at concentrations of (a) 150, (b) 300, (c) 600, and (d) 1200 ng/ μ L for 5 days. Release profiles show that ODN release depends on concentration of peptide amphiphile and ODN in the gel. Data points are average of $n = 3$ and error bars represent standard error of mean.

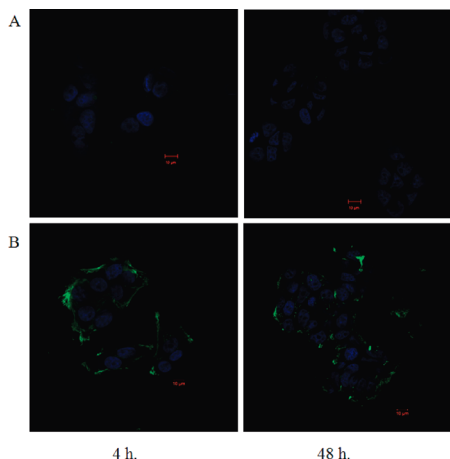


Figure 5. Representative images of MCF-7 cells treated with (A) naked FAM labeled ODN (green); (B) FAM-labeled ODN and 0.01 wt % PA complex for 4 h followed by an additional incubation of 44 h without treatment at 37 °C. TO-PRO-3 (blue) was used to stain the nuclei. PAs enhanced fluorescence intensity in cells significantly. Images were taken at 63 \times magnification.

therapy while providing elimination of side effects in the circulatory system after injection.

Incorporating ODNs into self-assembled Lys-PA nanofibers also enhanced ODNs' in vitro activity and their cellular uptake. Intracellular distribution of PA-ODN complexes was examined by laser scan confocal microscopy (Figure 4). MCF-7 cells were incubated with FAM labeled PA-ODN complex and free FAM labeled ODN for 4 h at 37 °C followed by fixation. In order to see

distribution of PA-ODN complexes in cell cytoplasm over time, cells were treated with PA-ODN including media for 4 h, after which medium was removed. Fresh cell culture medium was added and cells were incubated for an additional 44 h before fixation. After 48 h, we observed that PA-ODN complexes were internalized by cells (Figure 5). The internalization of ODN by cells continues through time, and thus, effectiveness of ODN is sustained. Stronger fluorescent intensity was observed in the cells treated with PA-ODN complex after both 4 h incubation and 48 h incubation with respect to ODN alone, indicating enhanced cellular uptake of ODN when it is applied with positively charged PA due to their amphiphilic and cationic properties.

To analyze the effects of PA-ODN complex on cell viability and proliferation, MTT viability and BrdU proliferation assays were carried out by using MCF-7 cells. Cells incubated with PA-ODN complex showed lower viability than cells incubated with ODN alone which proves that the PA nanofiber system is an effective delivery agent. Cells treated with PA-ODN complex also revealed lower viability compared to cells treated with PA-MM ODN complex, which shows that the decreased viability is not caused by the PA molecules. Proliferation assays revealed no significant differences between cells treated with ODN, MM-ODN, PA-ODN, and PA-MM ODN. This result is consistent with previously published data⁴⁶ (Figure S7a,b).

Functional delivery of ODN with PAs was also confirmed by real time PCR analysis that revealed PA and ODN (G3139) complex induced downregulation of the *Bcl-2* mRNA. MCF-7 cells treated with PA-ODN complex (G3139) exhibited a 70% downregulation in *Bcl-2* mRNA levels when compared to treatment groups with PA-mismatch ODN (G4126), ODN (G3139) alone, and mismatch ODN (G4126) alone when a 4 h long

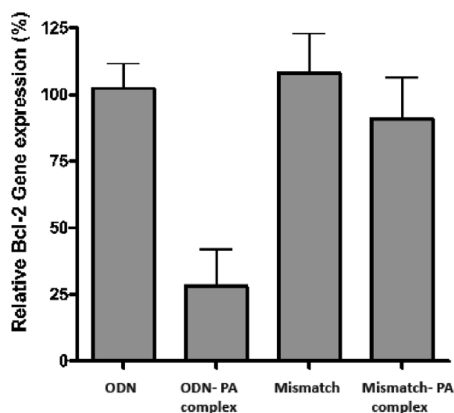


Figure 6. Effects of PA-ODN (G3139)/mismatch (G4126) complexes and free ODN/mismatch on mRNA levels of *Bcl-2* in MCF-7 breast cancer cells compared to cells incubated without ODN drug as change in gene expression (%). Total RNA was extracted from cells after 4 h of treatment followed by 44 h of incubation without treatment. GAPDH was used as housekeeping gene to normalize the gene expression level using Pfaffl method. Data points are average of $n = 3$ and error bars represent standard error of mean.

treatment was applied to cells followed by 44 h of incubation without treatment (Figure 6). At 72 h, downregulation of *Bcl-2* mRNA levels was around 30% for cells treated with PA-ODN complex, which was not significantly different than the other treatment groups (Figure S8). The increase in *Bcl-2* mRNA levels at 72 h compared to 48 h might be caused by development of resistance by MCF-7 cells against ODN treatment, similar to previously published data.⁴⁷ All expression levels were normalized to cells without any ODN treatment. These findings suggest that PAs can effectively deliver ODNs for gene-targeted therapies.

The effect of the *Bcl-2* antisense ODN (G3139) and its two base mismatch control (G4126) as naked and with Lys-PA on *Bcl-2* protein levels in MCF-7 cells were also examined with Western blot analysis, however, PA-ODN complex did not reveal any significant differences in *Bcl-2* protein levels compared to cells incubated with only cell culture medium (Figure S9). This result might be caused by the post-transcriptional and post-translational regulation mechanisms that are normally employed by cells to regulate protein levels and is a matter of effectiveness of G3139 itself. Nevertheless, the reduction in *Bcl-2* mRNA levels by itself at 48 h is sufficient to deduce that our delivery system enables effective delivery of the ODN agent.

All in vitro experiments were carried out with serum containing media in which most of the ODN carrier systems do not work.¹⁸ ODNs in the PA-ODN complexes are released by degradation of the biodegradable peptide scaffold. Synthesis and application of PAs as carrier and delivery agents have advantage of convenience in usage over other biodegradable polymers and lipids. Due to their biocompatibility, bioactive sequences, and highly ordered nanostructures, PA nanofibers are promising drug and gene delivery systems.

4. CONCLUSION

Development of carrier systems for controlled ODN release and efficient cellular uptake of ODNs is crucial for gene targeted therapy. In this study, we developed a novel carrier system consisting of peptide amphiphiles and antisense oligonucleotides

and analyzed the efficiency of controlled ODN release and delivery. The cationic Lys-PA molecule self-assembled upon addition of ODN and formed nanofibrous network in which oligonucleotides bind to peptide nanofibers through electrostatic interactions and form a stable complex. Our results demonstrate that ODN release profile depends on concentrations of the peptide amphiphile and ODN in the gel due to electrostatic attraction between cationic and anionic groups. 3D nanofiber network is also effective in encapsulation and release of ODN in a sustained manner. PA-ODN nanofibers delivered ODN efficiently and enhanced cellular uptake by MCF-7 cells, which resulted in downregulation of *Bcl-2* mRNA levels. Cationic Lys-PA provides a new tool for slow release and delivery of ODNs for gene targeted therapy. By combining apoptotic therapeutics and ODN treatment, PA nanofibers provide a promising tool for cancer treatment through loading peptide amphiphile gel with several drugs with different mechanisms of action to enhance apoptotic activity. PA nanofibrous system offers site-specific delivery of oligonucleotides by injectable gels applied to treatment site. Compared to intravenous administration, site specific delivery is expected to cause fewer side effects. In addition, this practical system can reduce the number of drug administrations, which cause patient discomfort and might lead to infections.

■ ASSOCIATED CONTENT

S Supporting Information. LC-MS results, self-supporting gel picture, additional ODN release graphs and in vitro results. This material is available free of charge via the Internet at <http://pubs.acs.org>.

■ AUTHOR INFORMATION

Corresponding Author

*E-mail: moguler@unam.bilkent.edu.tr; ttekinay@unam.bilkent.edu.tr; atekinay@unam.bilkent.edu.tr.

■ ACKNOWLEDGMENT

This work was supported by the Scientific and Technological Research Council of Turkey (TUBITAK) 110S018. We would like to thank Z. Erdogan for help in LC-MS and M. Guler for help in SEM. We are indebted to Genta Inc. for providing us the ODNs G3139, G4243, and G4126.

■ REFERENCES

- (1) Myers, K. J.; Dean, N. M. *Trends Pharmacol. Sci.* **2000**, *21*, 19–23.
- (2) Roehr, B. J. *Int. Assoc. Physicians AIDS Care* **1998**, *4*, 14–16.
- (3) Opalinska, J. B.; Gewirtz, A. M. *Nat. Rev. Drug Discovery* **2002**, *1*, 503–514.
- (4) Gray, G. D.; Basu, S.; Wickstrom, E. *Biochem. Pharmacol.* **1997**, *53*, 1465–1476.
- (5) Levin, A. A. *Biochim. Biophys. Acta* **1999**, *1489*, 69–84.
- (6) Hu, Q.; Shew, C. R.; Bally, M. B.; Madden, T. D. *Biochim. Biophys. Acta* **2001**, *1514*, 1–13.
- (7) Fimmel, S.; Saborowski, A.; Orfanos, C. E.; Zouboulis, C. C. *Horm. Res.* **2000**, *54*, 306.
- (8) Gref, R.; Minamitake, Y.; Peracchia, M. T.; Trubetskoy, V.; Torchilin, V.; Langer, R. *Science* **1994**, *263*, 1600–1603.
- (9) Singh, M.; Shirley, B.; Bajwa, K.; Samara, E.; Hora, M.; O'Hagan, D. *J. Controlled Release* **2001**, *70*, 21–28.
- (10) Mason, M.; Metters, A.; Bowman, C.; Anseth, K. *Macromolecules* **2001**, *34*, 4630–4635.

- (11) Hagan, S. A.; Coombes, A. G. A.; Garnett, M. C.; Dunn, S. E.; Davis, M. C.; Illum, L.; Davis, S. S.; Harding, S. E.; Purkiss, S.; Gellert, P. R. *Langmuir* **1996**, *12*, 2153–2161.
- (12) Kenawy, E. R.; Bowlin, G. L.; Mansfield, K.; Layman, J.; Sanders, E.; Simpson, D. G.; Wnek, G. E. *Abstr. Pap. Am. Chem. Soc.* **2002**, *223*, C115–C115.
- (13) Boussif, O.; Lezoualc'h, F.; Zanta, M.; Mergny, M.; Scherman, D.; Demeneix, B.; Behr, J. *Proc. Natl. Acad. Sci. U.S.A.* **1995**, *92*, 7297–7301.
- (14) Stewart, A. J.; Pichon, C.; Meunier, L.; Midoux, P.; Monsigny, M.; Roche, A. C. *Mol. Pharmacol.* **1996**, *50*, 1487–1494.
- (15) Walker, S.; Sofia, M. J.; Kakarla, R.; Kogan, N. A.; Wierichs, L.; Longley, C. B.; Bruker, K.; Axelrod, H. R.; Midha, S.; Babu, S.; Kahne, D. *Proc. Natl. Acad. Sci. U.S.A.* **1996**, *93*, 1585–1590.
- (16) Leong, K.; Mao, H.; Truong-Le, V.; Roy, K.; Walsh, S.; August, J. J. *J. Controlled Release* **1998**, *53*, 183–193.
- (17) Hemin Nie, L. Y. L.; Tong, H.; Wang, C.-H. *J. Controlled Release* **2008**, *129*, 207–214.
- (18) Summerton, J. E. *Ann. N.Y. Acad. Sci.* **2005**, *1058*, 62–75.
- (19) Claussen, R. C.; Rabatic, B. M.; Stupp, S. I. *J. Am. Chem. Soc.* **2003**, *125*, 12680–12681.
- (20) Niece, K. L.; Hartgerink, J. D.; Donners, J. J. M.; Stupp, S. I. *J. Am. Chem. Soc.* **2003**, *125*, 7146–7147.
- (21) Hartgerink, J. D.; Beniash, E.; Stupp, S. I. *Science* **2001**, *294*, 1684–1688.
- (22) Paramonov, S. E.; Jun, H. W.; Hartgerink, J. D. *J. Am. Chem. Soc.* **2006**, *128*, 7291–7298.
- (23) Jiang, H. Z.; Guler, M. O.; Stupp, S. I. *Soft Matter* **2007**, *3*, 454–462.
- (24) Stendahl, J. C.; Rao, M. S.; Guler, M. O.; Stupp, S. I. *Adv. Funct. Mater.* **2006**, *16*, 499–508.
- (25) Toksoz, S.; Mammadov, R.; Tekinay, A. B.; Guler, M. O. *J. Colloid Interface Sci.* **2011**, *356*, 131–137.
- (26) Bond, C. W.; Angeloni, N. L.; Harrington, D. A.; Stupp, S. I.; McKenna, K. E.; Podlasek, C. A. *J. Sex. Med.* **2011**, *8*, 78–89.
- (27) Hosseinkhani, H.; Hosseinkhani, M.; Khademhosseini, A.; Kobayashi, H. *J. Controlled Release* **2007**, *117*, 380–386.
- (28) Hosseinkhani, H.; Hosseinkhani, M.; Khademhosseini, A.; Kobayashi, H.; Tabata, Y. *Biomaterials* **2006**, *27*, 5836–5844.
- (29) Guler, M.; Claussen, R.; Stupp, S. *J. Mater. Chem.* **2005**, *15*, 4507–4512.
- (30) Accardo, A.; Tesauro, D.; Mangiapia, G.; Pedone, C.; Morelli, G. *Biopolymers* **2007**, *88*, 115–121.
- (31) Kim, J. K.; Anderson, J.; Jun, H. W.; Repka, M. A.; Jo, S. *Mol. Pharm.* **2009**, *6*, 978–985.
- (32) Hess, G. T.; Humphries, W. H. t.; Fay, N. C.; Payne, C. K. *Biochim. Biophys. Acta* **2007**, *1773*, 1583–1588.
- (33) Wiethoff, C. M.; Koe, J. G.; Koe, G. S.; Middaugh, C. R. *J. Pharm. Sci.* **2004**, *93*, 108–123.
- (34) Behanna, H. A.; Donners, J. J. M.; Gordon, A. C.; Stupp, S. I. *J. Am. Chem. Soc.* **2005**, *127*, 1193–1200.
- (35) He, C.; Hu, Y.; Yin, L.; Tang, C.; Yin, C. *Biomaterials* **2010**, *31*, 3657–3666.
- (36) Almofti, M. R.; Harashima, H.; Shinohara, Y.; Almofti, A.; Baba, Y.; Kiwada, H. *Arch. Biochem. Biophys.* **2003**, *410*, 246–253.
- (37) Beniash, E.; Hartgerink, J. D.; Storrer, H.; Stendahl, J. C.; Stupp, S. I. *Acta Biomater.* **2005**, *1*, 387–397.
- (38) Dai, G.; Chan, K. K.; Hoyt, D.; Whitman, S.; Klisovic, M.; Shen, T.; Caligiuri, M. A.; Byrd, J.; Grever, M.; Marcucci, G. *Clin. Cancer Res.* **2005**, *11*, 2998–3008.
- (39) Reed, J. *Hematol. Oncol. Clin. North Am.* **1995**, *9*, 451–473.
- (40) Youle, R. J.; Strasser, A. *Nat. Rev. Mol. Cell Biol.* **2008**, *9*, 47–59.
- (41) Rom, J.; von Minckwitz, G.; Marme, F.; Ataseven, B.; Kozyan, D.; Sievert, M.; Schlehe, B.; Schuetz, F.; Scharf, A.; Kaufmann, M. *Ann. Oncol.* **2009**, *20*, 1829–1835.
- (42) Moulder, S.; Symmans, W.; Booser, D.; Madden, T.; Lipsanen, C.; Yuan, L.; Brewster, A.; Cristofanilli, M.; Hunt, K.; Buchholz, T. *Clin. Cancer Res.* **2008**, *14*, 7909–7916.
- (43) Chi, K. N.; Gleave, M. E.; Klasa, R.; Murray, N.; Bryce, C.; Lopes de Menezes, D. E.; D'Aloisio, S.; Tolcher, A. W. *Clin. Cancer Res.* **2001**, *7*, 3920–3927.
- (44) Greenfield, N. J. *TrAC, Trends Anal. Chem.* **1999**, *18*, 236–244.
- (45) Greenfield, N.; Fasman, G. D. *Biochemistry* **1969**, *8*, 4108–4116.
- (46) Chi, K. C.; Wallis, A. E.; Lee, C. H.; De Menezes, D. L.; Sartor, J.; Dragowska, W. H.; Mayer, L. D. *Breast Cancer Res. Treat.* **2000**, *63*, 199–212.
- (47) Lopes de Menezes, D. E.; Hudon, N.; McIntosh, N.; Mayer, L. D. *Clin. Cancer Res.* **2000**, *6*, 2891–2902.